JOURNAL OF MATERIALS SCIENCE 25 (1990) 522–528

A statistical evaluation of the free energy of Fe-base ternary ordering alloys

MASUHIRO FUKAYA, TORU MIYAZAKI, PI ZHI ZHAO, TAKAO KOZAKAI
Department of Materials Science and Engineering, Nagoya Institute of Technology, Gokiso-cho, Showa-ku, Nagoya 466, Japan

The free energy of the Fe-base ternary ordering alloys where $B2$ and $D0_3$ ordered structures are formed is evaluated. The statistical theory is employed using a pairwise interaction approximation taking into account not only the atomic interaction but also the magnetic interaction, based upon the Bragg–Williams–Gorsky model. The application of this model on Fe–Si–Co ordering alloys are demonstrated. The propriety of the calculation results are performed by comparing the experimental results. The influences of the magnetic energy to the stability of ordered structures are also demonstrated.

1. Introduction

It has been recognized so far that the phase separation of the supersaturated solid solution occurs only in the alloy systems having the positive interaction parameter between the nearest neighbour atoms. Recently, however, several experimental studies have revealed that the phase separation actually occurs in the ordering solid solutions such as Fe–Al [1–6], Fe–Si [7–10], Cu–Zn [11, 12], Cu–Mn–Al [13] and several Fe-base ternary ordering alloys [14–18], which have negative interaction parameters. Therefore, the experimental facts above described have urged us to change the conventional concept that the phase separation type alloy and the ordering type alloy have opposite characteristics. In order to understand the solute atom segregation in ordering alloy, it is important to evaluate the free energies of ordered and disordered solid solutions precisely. For the binary ordering alloys, theoretical pursuits [19–38] have been proposed by taking into account the interatomic interactions between not only the nearest neighbours but also the second and the higher order neighbours. In the theoretical treatment of this sort, even if the first order interaction parameter is negative, phase separations are expected to occur when the second and the higher order interaction parameters are positive.

As regards ternary ordering alloys, we have already found that the two phase regions exist in the Fe-rich ternary ordering alloys, e.g. Fe–Si–Al [14], Fe–Al–Co [15], Fe–Si–V [16], Fe–Si–Co [16] and so on. However, the theoretical investigation for the ternary ordering systems has scarcely been performed so far, possibly because of the laborious descriptions of $B2$ and $D0_3$ ordered structures in the ternary alloy systems. However for the theoretical justification of experimental results the evaluation of free energies of the $B2$ and $D0_3$ ordered structures is important.

In the present paper, firstly we propose the evaluation method of the free energy of Fe-base ternary $B2$ and $D0_3$ ordered structures. Secondly applying the free energy model on the Fe–Si–Co ordering alloys, we show the most stable ordered structures, and discuss the propriety of the proposed free energy model.

2. Theoretical basis

2.1. Descriptions of $B2$ and $D0_3$ ordered structures in the A-B-C ternary ordering system

In order to describe the atomic configurations of $B2$ and $D0_3$ ordered structures in b.c.c ternary alloy, the unit cell of the $D0_3$ superlattice is divided into four f.c.c. sublattices I, II, III, IV, as illustrated in Fig. 1. The atoms in the sublattice I and II are the nearest neighbours (n.n.) to the atoms in the sublattice III and IV. The atoms in the I or III sublattice are the second nearest neighbours (n.n.n.) to the atoms in the II or IV respectively. To describe the various atomic configurations in the first and second coordination spheres of the b.c.c. ternary alloys, we use six independent parameters defined by occupation probabilities P_i^L of i atom ($i = A, B$) in the sublattice $L(=\mathrm{I, II, III, IV})$, similarly as the case of binary alloys [22, 27]:

$$\begin{aligned}
X_A &= \frac{(P_A^{\mathrm{I}} + P_A^{\mathrm{II}} - P_A^{\mathrm{III}} - P_A^{\mathrm{IV}})}{(P_A^{\mathrm{I}} + P_A^{\mathrm{II}} + P_A^{\mathrm{III}} + P_A^{\mathrm{IV}})} \\
Y_A &= \frac{(P_A^{\mathrm{III}} - P_A^{\mathrm{IV}})}{(P_A^{\mathrm{III}} + P_A^{\mathrm{IV}})} \\
Z_A &= \frac{(P_A^{\mathrm{I}} - P_A^{\mathrm{II}})}{(P_A^{\mathrm{I}} + P_A^{\mathrm{II}})} \\
X_B &= \frac{(P_B^{\mathrm{I}} + P_B^{\mathrm{II}} - P_B^{\mathrm{III}} - P_B^{\mathrm{IV}})}{(P_B^{\mathrm{I}} + P_B^{\mathrm{II}} + P_B^{\mathrm{III}} + P_B^{\mathrm{IV}})} \\
Y_B &= \frac{(P_B^{\mathrm{III}} - P_B^{\mathrm{IV}})}{(P_B^{\mathrm{III}} + P_B^{\mathrm{IV}})} \\
Z_{\mathrm{B}} &= \frac{(P_B^{\mathrm{I}} - P_B^{\mathrm{II}})}{(P_B^{\mathrm{III}} + P_B^{\mathrm{IV}})} \qquad (1)
\end{aligned}$$

The parameters X_A and X_B indicate the atomic con-

0022-2461/90 $03.00 + .12

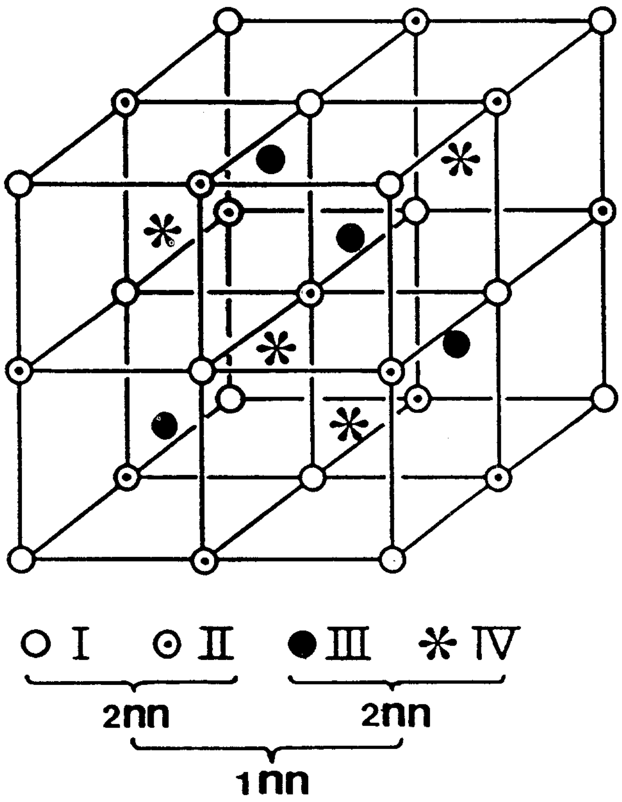

Figure 1 Unit cell of $D0_3$ structure and four f.c.c. sublattices, indicating the nearest (n.n.) and second nearest (n.n.n.) neighbourhood between atom sites of the sublattices I, II, III, IV.

figurations of A and B atoms between the nearest neighbour sites, i.e. between the sublattices (I + II) and (III + IV). Similarly, other order parameters Y_A, Y_B, Z_A and Z_B show the atomic configurations of A and B atoms between the second nearest neighbour sites, i.e. between the sublattices I and II and also between the sublattices III and IV. All parameters vary in a range of $-1 \leqq X_i, Y_i, Z_i \leqq 1$ $(i = A, B)$. The configurations of C atoms would be inevitably determined by the parameters X_i, Y_i and Z_i $(i = A, B)$. The uniform distribution of the atoms onto the four sublattices is given by a condition of $X_A = Y_A = Z_A = X_B = Y_B = Z_B = 0$. When $Y_A = Y_B = Z_A = Z_B = 0$ and $X_A \neq 0$ or $X_B \neq 0$, the sublattice I and II are preferentially occupied by A atom or B atom respectively. Therefore, by assuming that atoms are distributed at random in each sublattice, the amount of unlike atom pare of the nearest neighbour increases, i.e. the progress of $B2$ ordering. Similarly, when one of the parameter X_i $(i = A, B)$ is not zero at least and also one of the parameters Y_i and Z_i $(i = \mathrm{A}, \mathrm{B})$ is not zero at least, unlike atom pares between the 2nd neighbour sites increase in number. This gives rise to the development of $D0_3$ ordering. On the basis of the above consideration, the $A2$, $B2$, $D0_3$ and $B32$(NaTl) structures of A-B-C ternary system can generally be expressed by using the six ordering parameters as follows:

$A2$: random distribution atoms in the nearest neighbour sites (n.n.) and the 2nd nearest neighbour sites (n.n.n.)

$$X_A^2 + X_B^2 = 0, \; Y_A^2 + Y_B^2 = 0, \; Z_A^2 + Z_B^2 = 0 \qquad (2)$$

$B2$: ordering in the n.n. and random distribution in the n.n.n.

$$X_A^2 + X_B^2 \neq 0, \; Y_A^2 + Y_B^2 = 0, \; Z_A^2 + Z_B^2 = 0 \qquad (3)$$

$D0_3$: ordering in the n.n. and the n.n.n.

$$X_A^2 + X_B^2 \neq 0, \; Y_A^2 + Y_B^2 \overset{=}{\underset{\neq}{\neq}} 0, \; Z_A^2 + Z_B^2 \overset{\neq}{\underset{=}{\neq}} 0 \qquad (4)$$

$B32$: random distribution in the n.n. and ordering in the n.n.n.

$$X_A^2 + X_B^2 = 0, \; Y_A^2 + Y_B^2 \neq 0, \; Z_A^2 + Z_B^2 \neq 0 \qquad (5)$$

The structural factors of X-ray diffraction for the $A2$, $B2$ and $D0_3$ structures of the ternary system can be evaluated by using the six ordering parameters. In the present the reflection spots are labelled by indices for the unit cell of the $D0_3$ ordered lattice (see Fig. 1). The ordering in the n.n. is proved by exciting the 200 superlattice refraction and the ordering in the n.n.n. is proved by the 111. The structural factors for each reflection are described as follows:

$$|F(220)|^2 = 16^2(C_A f_A + C_B f_B + C_C f_C)^2 \qquad (6)$$

$$|F(200)|^2 = 16^2[C_A(f_A - f_C)X_A + C_B(f_B - f_C)X_B]^2 \qquad (7)$$

$$\begin{aligned}|F(111)|^2 = 8^2\{&[C_A(f_A - f_C)(1 + X_A)Z_A \\ &+ C_B(f_B - f_C)(1 + X_B)Z_B]^2 \\ &+ [C_A(f_A - f_C)(1 - X_A)Y_A \\ &+ C_B(f_B - f_C)(1 - X_B)Y_B]^2\}\end{aligned} \qquad (8)$$

In these equations, C_A, C_B and C_C = chemical concentrations of A, B and C atoms, f_A, f_B and f_C = atomic scattering factors of A, B and C atoms, X_i, Y_i and $Z_i (i = A, B)$ = the ordering parameters defined by Equation 1.

When the $B2$ structure exists, the 200 super lattice refractions appear without 111 reflection, because the ordering parameter X_A or X_B is not zero but Y_A, Y_B, Z_A and Z_B are zero, as is clearly known from the Equation 3. Similarly, if the $D0_3$ structure exists, the 111 super lattice refraction appears in addition to the 200 spot. When the disordered phase exists the super lattice refraction does not appear, because all ordering parameters are zero. Thus, it is obvious that the atomic configurations of the ternary ordering, defined by Equations 2–5 are related to the electron diffraction patterns experimentally observed [14–18].

2.2. Descriptions of *ferro*- and *para*-magnetic states in the *A*-*B*-*C* ternary system

The magnetic interactions are derived by considering the pairwise interactions [23, 39]. The magnetic spin is assumed to have just up or down state, regardless of various values of the actual magnetic moment. Therefore there are only two separate energy states $V_{ij}^{(1)}$ and $V_{ij}^{(1)}$ of i-j atom pairs with parallel and anti-parallel spins, respectively. The following relations hold;

$$V^{(1)}_{i\uparrow j\uparrow} = V^{(1)}_{i\downarrow j\downarrow} \tag{9}$$

and

$$V^{(1)}_{i\uparrow j\downarrow} = V^{(1)}_{i\downarrow j\uparrow} \tag{10}$$

The higher order of the magnetic interactions such as the second nearest neighbour is neglected. The occupation probabilities of the i atom ($i = A$, B, C) with up spin or down spin onto the sublattice $L(=\mathrm{I}$, II, III, IV) are given by

$$P^L_{i\uparrow} = \frac{P^L_i(1 + q_i)}{2} \text{ or } P^L_{i\downarrow} = \frac{P^L_i(1 - q_i)}{2} \tag{11}$$

respectively. $P^L_i(=P^L_{i\uparrow} + P^L_{i\downarrow})$ is the probability of existence for the component i in the sublattice L. In Equation 11 $(1 + q_i)/2$ and $(1 - q_i)/2$ are the probabilities of existence of the i atom having up spin and down spin respectively. The *para*-magnetic state could be expressed by Equation 12:

$$\left(\frac{1 + q_i}{2}\right) = \left(\frac{1 - q_i}{2}\right) = 0.5 \tag{12}$$

Here q_i represents the distribution of magnetic spins, varying in a range of $0 \leqq q_i \leqq 1$. The *ferro*-magnetic and *para*-magnetic states are shown by $q_i = 1$ and $q_i = 0$ respectively.

2.3. Free energies of Fe-base ternary $B2$ and $D0_3$ ordered structures

On the basis of the Bragg-Williams-Gorsky (B.W.G.) approximation [40, 41], the configurational free energy F_k of the A-B-C ternary system containing *ferro*-magnetic elements is given by Equation 13.

$$F_k = \sum_k \sum_i \sum_j N^{(k)}_{ij} V^{(k)}_{ij} - T(S_C + S_q) \tag{13}$$

where $N^{(k)}_{ij}$ = the number of atom pairs between i and j atoms, $V^{(k)}_{ij}$ = the bond energy between i and j atom in the k'th neighbours, T = temperature, S_C = the chemical part of the configurational entropy, S_q = the magnetic part of the configurational entropy. The chemical part of the configurational entropy is given by

$$S_C = \frac{-k_B N}{4} \sum_L \sum_i P^L_i \ln P^L_i \tag{14}$$

where k_B = Boltzman's constant, N = Abogadoro number (the number of all lattice sites). The atomic interchange energies of the k'th neighbours $W_{ij}(k)$ are deduced from the chemical bond energies;

$$W^{(k)}_{ij} = -2V^{(k)}_{ij} + V^{(k)}_{ii} + V^{(k)}_{jj} \tag{15}$$

where the positive $W^{(k)}_{ij}$ corresponds to larger affinity between the unlike atom pair than the like pair, i.e. the ordering tendency exists. Since the average of bong energy in the *para*-magnetic i–j crystal is given by

$$V^{(1)}_{ij} = 0.5[V^{(1)}_{i\uparrow j\uparrow} + V^{(1)}_{i\uparrow j\downarrow}] \tag{16}$$

the magnetic parameter $J^{(1)}_{ij}$ is defined by Equations 17 and 18.

$$V^{(1)}_{i\uparrow j\uparrow} = V^{(1)}_{ij} + J^{(1)}_{ij} \tag{17}$$

$$V^{(1)}_{i\uparrow j\downarrow} = V^{(1)}_{ij} - J^{(1)}_{ij} \tag{18}$$

In the form of Equations 17 and 18 *ferro*-magnetism occurs when $J^{(1)}_{ij} < 0$. For the sake of simplicity, the magnetic interchange energies $J^{(1)}_{ij}$ as well as the atomic interchange energies $W^{(k)}_{ij}$ are assumed to be independent of temperature, composition and distribution of atoms [22, 39]. The number of the atom pairs in the first and second nearest neighbours are given by Equations 19 and 20, respectively.

$$\begin{aligned} N^{(1)}_{ij} = {} & a_{ij}N[(P^{\mathrm{I}}_i + P^{\mathrm{II}}_i)(P^{\mathrm{III}}_j + P^{\mathrm{IV}}_j) \\ & + (P^{\mathrm{III}}_i + P^{\mathrm{IV}}_i)(P^{\mathrm{I}}_j + P^{\mathrm{II}}_j)] \end{aligned} \tag{19}$$

$$N^{(2)}_{ij} = a_{ij}\frac{3N}{2}(P^{\mathrm{I}}_i P^{\mathrm{II}}_j + P^{\mathrm{II}}_i P^{\mathrm{I}}_j + P^{\mathrm{III}}_i P^{\mathrm{IV}}_j + P^{\mathrm{IV}}_i P^{\mathrm{III}}_j) \tag{20}$$

$$a_{ij} = 1 \quad \text{for} \quad i \neq j$$

$$a_{ij} = 0.5 \quad \text{for} \quad i = j$$

and

$$i, j = A\uparrow, A\downarrow, B\uparrow, B\downarrow, C\uparrow, C\downarrow.$$

The probabilities P^L_i in these equations are expressed by using the magnetic order parameters q_A, q_B and the chemical order parameters X_A, X_B, Y_A, Y_B, Z_A, Z_B:

$$\begin{aligned} P^{\mathrm{I}}_A &= C_A(1 + X_A)(1 + Z_A) \\ P^{\mathrm{II}}_A &= C_A(1 + X_A)(1 - Z_A) \\ P^{\mathrm{III}}_A &= C_A(1 - X_A)(1 + Y_A) \\ P^{\mathrm{IV}}_A &= C_A(1 - X_A)(1 - Y_A) \\ P^L_{A\uparrow} &= \frac{P^L_A(1 + q_A)}{2} \\ P^L_{A\downarrow} &= \frac{P^L_A(1 - q_A)}{2} \\ P^{\mathrm{I}}_B &= C_B(1 + X_B)(1 + Z_B) \\ P^{\mathrm{II}}_B &= C_B(1 + X_B)(1 - Z_B) \\ P^{\mathrm{III}}_B &= C_B(1 - X_B)(1 + Y_B) \\ P^{\mathrm{IV}}_B &= C_B(1 - X_B)(1 - Y_B) \\ P^L_{B\uparrow} &= \frac{P^L_B(1 + q_B)}{2} \\ P^L_{B\downarrow} &= \frac{P^L_B(1 - q_B)}{2} \\ L &= \mathrm{I, II, III, IV} \end{aligned}$$

where C_A = atomic concentration of A, C_B = atomic concentration of B, C_C = atomic concentration of C.

According to Semenovskaya [29], the magnetic part of the configurational entropy S_q has been derived as follows:

$$\begin{aligned} S_q = {} & k_B N \sum_i C_i\{\ln(8 - 6q_i + 2\sqrt{4 - 3q_i^2}) \\ & - (1 + q_i)\ln(q_i + \sqrt{4 - 3q_i^2}) \\ & - (1 - q_i)\ln[2(1 - q_i)]\} \end{aligned} \tag{22}$$

Consequently, the configurational free energy of A-B-C ternary system containing *ferro*-magnetic elements can be expressed by Equation 23

$$\begin{aligned}
F_k = {} & U^0 - N\sum_{ij} C_i C_j\{4[W_{ij}^{(1)} + M_{ij}^{(1)}] + 3W_{ij}^{(2)}\} \\
& + 4N\sum_i C_i J_{ij}^{(1)} q_i^2 + N\sum_{ij} C_i C_j X_i X_j \\
& \times \{4[W_{ij}^{(1)} + M_{ij}^{(1)}] - 3W_{ij}^{(2)}\} \\
& + \frac{3N}{2}\sum_{ij} C_i C_j[(1 - X_i)(1 - X_j)Y_i Y_j \\
& + (1 + X_i)(1 + X_j)Z_i Z_j]W_{ij}^{(2)} \\
& + kNT\sum_i C_i \ln C_i + \frac{kNT}{2}\sum_i C_i\{(1 - X_i) \\
& \times \ln(1 - X_i) + (1 + X_i)\ln(1 + X_i)\} \\
& + \frac{kNT}{4}\sum_i \{C_i(1 - X_i)[(1 + Y_i)\ln(1 + Y_i) \\
& + (1 - Y_i)\ln(1 - Y_i)] \\
& + C_i(1 + X_i)[(1 + Z_i)\ln(1 + Z_i) \\
& + (1 - Z_i)\ln(1 - Z_i)]\} \\
& - kNT\sum_i m_i C_i\{\ln(8 - 6q_i + 2\sqrt{4 - 3q_i^2}) \\
& - (1 + q_i)\ln(q_i + \sqrt{4 - 3q_i^2}) \\
& - (1 - q_i)\ln[2(1 - q_i)]\}
\end{aligned}$$

where

$$\begin{aligned}
U^0 &= N\left(4\sum_i C_i V_{ii}^{(1)} + 3\sum_i C_i V_{ii}^{(2)}\right) \\
M_{ij}^{(1)} &= -2J_{ij}^{(1)} q_i q_j + J_{ii}^{(1)} q_i^2 + J_{jj}^{(1)} q_j^2 \\
ij &= AB,\ BC,\ CA \\
i &= A,\ B,\ C \\
m_A &= m_B = m_C = 1 \text{ if } J_{AA}^{(1)} \neq 0
\end{aligned}$$

and

$$\begin{aligned}
J_{BB}^{(1)} &\neq 0 \quad \text{and} \quad J_{CC}^{(1)} \neq 0 \\
m_A &= 0 \quad \text{if } J_{AA}^{(1)} = 0 \\
m_B &= 0 \quad \text{if } J_{BB}^{(1)} = 0 \\
m_C &= 0 \quad \text{if } J_{CC}^{(1)} = 0
\end{aligned} \tag{23}$$

m_i = a parameter to qualify the *ferro*-magnetic energy with i-element, which is usually unit in the case where i is *ferro*-magnetic element.

In Equation 23 U^0 is the bonding energy term of pure components, which is not significant for the order–disorder phase transitions. The second term is the energy of mixing, the third term is the internal energy due to the *ferro*-magnetic components, the fourth and fifth terms show the energy contribution arising from the atomic ordering in the n.n. and in the n.n.n., respectively. The last term in Equation 23 is entropy contribution. Thus, the configurational free energy is now evaluated.

3. Applications to the Fe–Si–Co ordering system

3.1. Calculation method

The most stable configuration of the phases was determined by numerical calculations in computer, using the energy parameters $W_{ij}^{(k)}$ ($k = 1, 2$) and $J_{ij}^{(1)}$. The numerical values used for the calculation are listed in the following, which have already been given by Inden [28, 42] for the binary systems the structure determined on the basis of the B.W.G. model.

$$\begin{aligned}
W_{\mathrm{FeSi}}^{(1)} &= 2010\,k_{\mathrm{B}}\,\mathrm{J\,mol^{-1}} \\
W_{\mathrm{FeCo}}^{(1)} &= 410\,k_{\mathrm{B}}\,\mathrm{J\,mol^{-1}} \\
W_{\mathrm{SiCo}}^{(1)} &= 2600\,k_{\mathrm{B}}\,\mathrm{J\,mol^{-1}} \\
W_{\mathrm{FeSi}}^{(2)} &= 1000\,k_{\mathrm{B}}\,\mathrm{J\,mol^{-1}} \\
W_{\mathrm{FeCo}}^{(2)} &= 0\,\mathrm{k}_B\,\mathrm{J\,mol^{-1}} \\
W_{\mathrm{SiCo}}^{(2)} &= 700\,k_{\mathrm{B}}\,\mathrm{J\,mol^{-1}} \\
J_{\mathrm{FeFe}}^{(1)} &= -196\,k_{\mathrm{B}}\,\mathrm{J\,mol^{-1}} \\
J_{\mathrm{CoCo}}^{(1)} &= -261\,k_{\mathrm{B}}\,\mathrm{J\,mol^{-1}} \\
J_{\mathrm{FeCo}}^{(1)} &= -296\,k_{\mathrm{B}}\,\mathrm{J\,mol^{-1}}
\end{aligned}$$

The stable configuration of ordered phases was numerically calculated using the steepest decent method. If the numerical calculation gives a specified solution of the order parameters, this value corresponds to the most stable atomic configurations. As an example, the ordering excess energy F^{ord} is plotted in Fig. 2a to c for the Fe-5 at % Si-5 at % Co, Fe-10 at % Si-13 at % Co and Fe-18 at % Si-16 at % Co alloys at 823 K with respect to only the chemical order parameter. The minimum point of F^{ord} in the coordinate system of the order parameter is indicated by $X_A$min, $X_B$min, $Z_A$min and $Z_B$min. In Fig. 2 the description of F^{ord} with respect to $Y_i (i = A, B)$ is omitted, because the $Y_A$min and $Y_B$min are always zero to 823 K. The F^{ord} with $Z_i (i = A, B)$ are calculated under the condition of the fixed $X_A$min and $X_B$min. In a case of the Fe-5 at % Si-5 at % Co alloy shown in Fig. 2a the order parameters $X_A$min, $X_B$min, $Z_A$min and $Z_A$min are zero, indicating that the disordered configuration, i.e. A2 structure, is most stable. However with increase of the solute content so as to exceed a certain critical composition, the parameters $X_A$min and $X_B$min move from zero. In Fig. 2b for the Fe-10 at % Si-13 at % Co alloy the $X_A\text{min} = 0.75$, $X_B\text{min} = -0.35$, $Z_A\text{min} = 0$ and $Z_B\text{min} = 0$. These parameters show that the $B2$ structure is stable in this case, because the ordering exists only in the nearest neighbour bond. In the high solute content alloy the parameters $Z_i$min also become non-zero, as can be seen in Fig. 2c; $X_A\text{min} = 0.99$, $X_B\text{min} = -0.76$, $Z_A\text{min} = 0.95$ and $Z_B\text{min} = -0.24$. The $D0_3$ configuration is most stable.

3.2. Configuration diagrams of the Fe–Si–Co system

Fig. 3 shows the configuration diagram calculated at 823 K, which shows the most stable atomic configurations of the homogeneous solid solutions. The solid curves indicate the phase boundaries of $A2/B2$ and $B2/D0_3$, respectively. The $D0_3$ structure is stable in the composition range more than 12 at % Si. The dotted

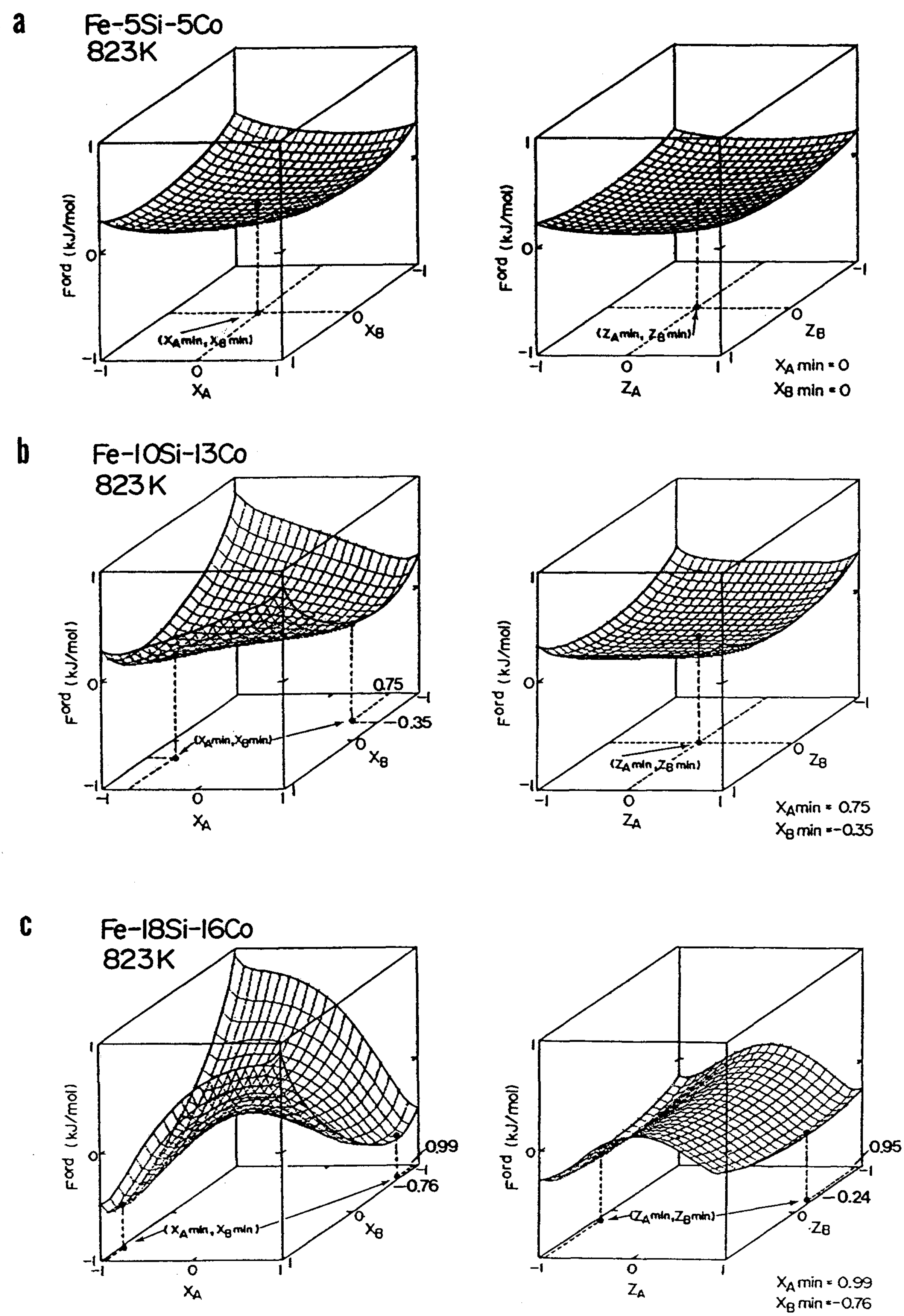

Figure 2 Configurational part of the free energy with respect to the order parameters X_A, X_B, Z_A, Z_B calculated for Fe-5 at % Si-5 at % Co (a), Fe-10 at % Si-13 at % Co (b) and Fe-18 at % Si-16 % Co (c), at 823 K.

curve in Fig. 3 shows the change of Curie temperature (Tc) with composition. Therefore, $A2$ and $B2$ structures are *ferro*-magnetic at 823 K, while $D0_3$ structure is in *ferro*-magnetic or *para*-magnetic state. Fig. 4 represents equi-Curie temperatures calculated for various temperatures from 723 K to 1 323 K. The Curie temperature, having a summit at about Fe-50 at % Co, decreases with increasing Si content.

4. Discussion

The calculated diagram is compared with the experimentally obtained one. Fig. 5 is an isothermal Fe–Si–

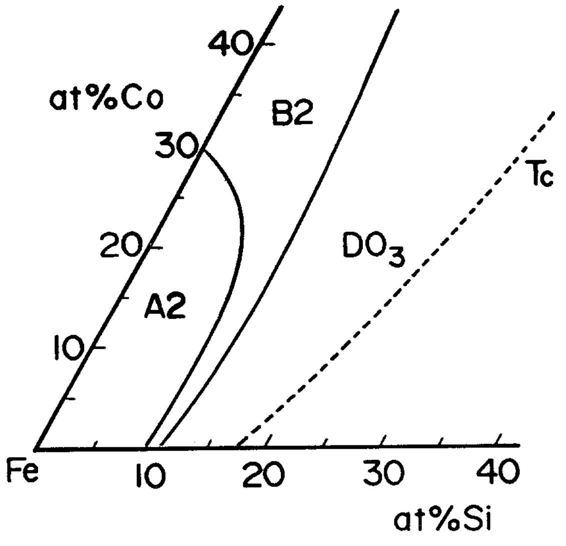

Figure 3 An isothermal configuration diagram calculated for Fe-rich Fe–Si–Co ternary system at 823 K.

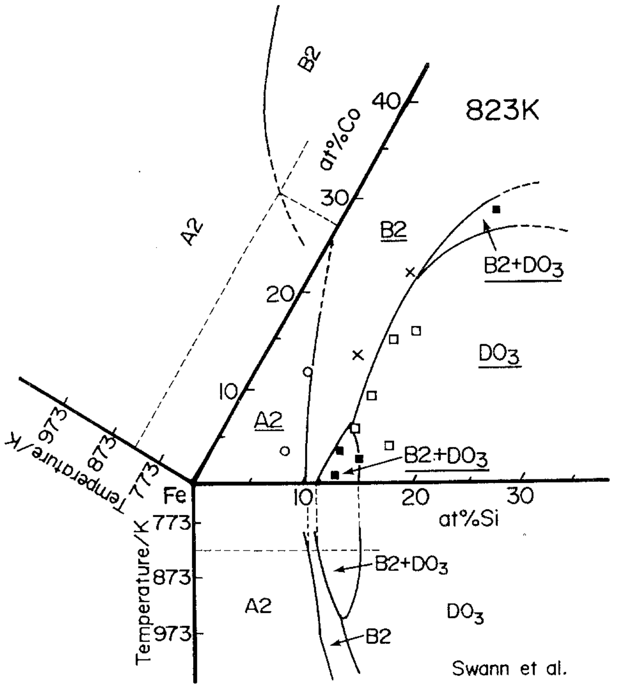

Figure 5 An isothermal section phase diagram of Fe-rich Fe–Si–Co ternary system at 823 K together with Fe–Si and Fe–Co binary phase diagrams, ○ = $A2$ phase, × = $B2$ phase, □ = $D0_3$ phase and ■ = $B2 + D0_3$ phase [16].

Co phase diagram at 823 K with Fe–Si and Fe–Co binary phase diagrams, which was experimentally obtained [16]. This figure shows the existence of $A2$, $B2$ and $D0_3$ single phase regions and also coexistent regions of $B2 + D0_3$. The boundaries of $A2/B2$ and $B2/D0_3$ transitions in the calculated configuration diagram (Fig. 3) are seemed to be consistent with the experimentally obtained one (Fig. 5). Fig. 6 shows the Curie temperatures experimentally obtained for the various Fe–Si–Co ternary alloys. Other researcher's work [42] is also represented in Fig. 6. It should be noted that the experimental Curie temperatures are fairly well consistent with the theoretical temperatures shown in Fig. 4.

In order to know the influence of the *ferro*-magnetism on the ordered structures, the configuration diagram of the pure *para*-magnetic states ($qA = qB = 0$) is given in Fig. 7. The solid curves show the $A2/B2$ and $B2/D0_3$ transitions for the *para*-magnetic state. The phase transition of *ferro*-magnetic state are also described in dotted curves. It should be noticed that the *ferro*-magnetism produces the drastic contraction of disorder $A2$ region, that is drastic expansion of $B2$ region as can be seen in the low Si and high Co composition area, while the $B2$ region shrinks, although slightly, in the composition area of 10 ~ 20 at % Co and 10 at % Si. Thus the expansion of the $B2$ region, i.e. the stabilization of $B2$ structure is considered to be due to the large magnetic contribution to the Fe–Co n.n. bond, as compared with that to the Fe–Fe or Co–Co n.n. bonds. On the other hand, the destabilization of $B2$ structure which is seen in the low Co composition area is caused by the additional magnetic strength to the Fe–Fe n.n. bonds. Since the $B2/D0_3$ transition in the figure is scarcely moved by

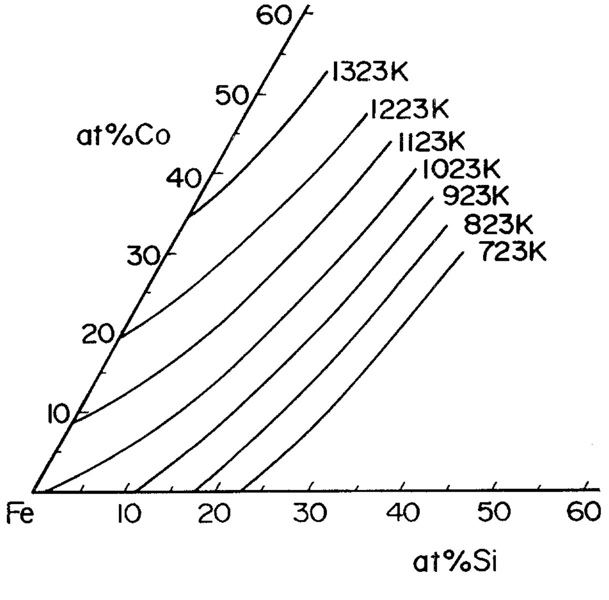

Figure 4 The contour map of equi-Curie temperatures calculated for Fe-rich Fe–Si–Co ordering system.

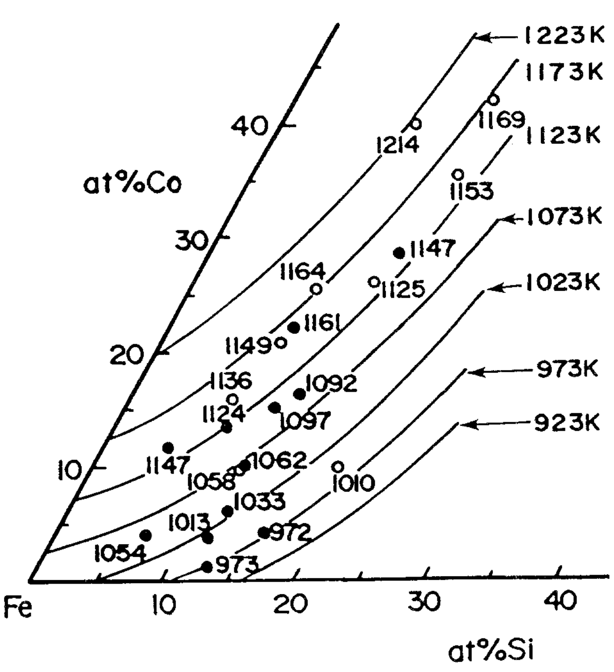

Figure 6 Measured Curie temperatures of Fe–Si–Co alloys, ● = this work, ○ = Inden [42] and the contour map of equi-Curie temperatures.

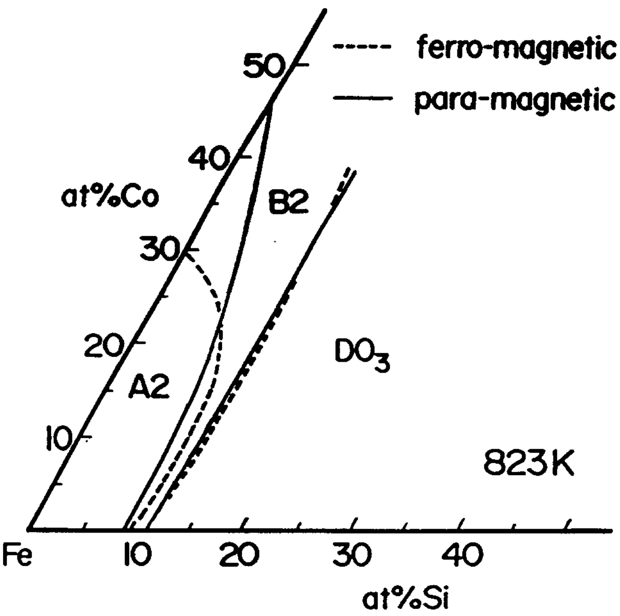

Figure 7 The calculated configuration diagrams of both *para*-magnetic and *ferro*-magnetic states, respectively, to demonstrate the influences of the *ferro*-magnetism to ordered structures.

the additional magnetic energy, the DO_3 structure seemed to be less effected by the magnetic energy, compared with the case of $B2$ structure.

From the free energy of the most stable states the phase diagram is easily obtained by the common tangent contraction with different compositions and different degrees of order. The theoretical investigations on the phase diagrams will be reported in the near future.

5. Conclusions

The free energy of Fe-base ternary ordering alloys where the $B2$ and $D0_3$ ordered structures were formed was evaluated on the basis of the statistical approach of the Bragg–Williams–Gorsky approximation. The magnetic interaction was also taken into account. The configuration diagrams of Fe–Si–Co ternary ordering system were calculated and compared with the experimental results to show the propriety of the calculated results. The influences of the magnetic energy on the structural stability of ordered phases are also demonstrated. The theoretical description proposed in the present study is useful for the thermodynamic implication of the equilibrium phase diagrams.

Acknowledgements

The authors are grateful to Dr. M. Doi of the Nagoya Institute of Technology.

This work was financially supported in part by Grant-in-Aid for Scientific Research Fund from the Ministry of Education, Science and Culture, Japan.

References

1. S. M. ALLEN and J. W. CAHN, *Acta Metall.* **23** (1975) 1017.
2. S. M. ALLEN, *Phil. Mag.* **36** (1977) 181.
3. P. R. SWANN, W. R. DUFF and R. M. FISHER, *Trans. Met. Soc. AIME.* **245** (1969) 851.
4. P. R. SWANN, W. R. DUFF and R. M. FISHER, *Metall. Trans.* **3** (1972) 409.
5. K. OKI, H. SAGANE and T. EGUCHI, *Jpn J. Appl. Phys.* **13** (1974) 753.
6. H. SAGANE, K. OKI and T. EGUCHI, *Trans. JIM.* **18** (1977) 488.
7. G. INDEN and W. PITSCH, *Z. Metallkde* **63** (1972) 253.
8. H. H. ETTWIG and W. PEPPERHOFF, *ibid.* **63**, (1972) 453.
9. G. SCHLATTE and W. PITSCH, *ibid.* **66** (1975) 660.
10. P. R. SWANN, L. GRÅNÄS and B. LEHTINEN, *Metal Sci.* **9** (1975) 90.
11. H. KUBO and C. M. WAYMAN, *Metall. Trans.* **10A** (1979) 633.
12. H. KUBO, I. CORNELIS and C. M. WAYMAN, *Acta Metall.* **28** (1980) 405.
13. M. BOUCHARD and G. THOMAS, *ibid.* **23** (1975) 1485.
14. T. MIYAZAKI, T. KOZAKAI and T. TSUZUKI, *J. Mater. Sci.* **21** (1986) 2557.
15. T. MIYAZAKI, K. ISOBE, T. KOZAKAI and M. DOI, *Acta Metall.* **35** (1987) 317.
16. M. FUKAYA, T. KOZAKAI and T. MIYAZAKI, *J. Jpn Inst. Metal.* **52** (1988) 369 (in Japanese).
17. S. MATSUMURA, A. SONOBE, K. OKI and T. EGUCHI, in Proceedings International Conference. "Phase Transformations in Solids", (Elsevier, New York, 1984) **21**, 269.
18. M. G. MENDIRATTA, S. K. EHLERS and H. A. LIPSITT, *Metall. Trans.* **18A** (1987) 509.
19. P. S. RUDMAN, *Acta Metall.* **8** (1960) 321.
20. W. C. RICHARDS and J. W. CAHN, *ibid.* **19** (1971) 1263.
21. S. M. ALLEN and J. W. CAHN, *ibid.* **20** (1972) 423.
22. G. INDEN and W. PITSCH, *Z. Metallkde* **62** (1971) 627.
23. G. SCHLATTE, G. INDEN and W. PITSCH, *ibid.* **65** (1974) 94.
24. G. INDEN and W. PITSCH, *ibid.* **67** (1976) 462.
25. G. INDEN, *Acta Metall.* **22** (1974) 945.
26. *Idem Z. Metallkde* **66** (1975) 577.
27. *Idem, ibid.* **66** (1975) 648.
28. *Idem, ibid.* **68** (1977) 529.
29. S. V. SEMENOVSKAYA, *Phys Status Solidi* **64(b)** (1974) 291.
30. S. V. SEMENOVSKAYA and D. M. UMIDOV, *ibid.* **64(b)** (1974) 627.
31. R. KIKUCHI and C. M. VAN BAAL, *Scripta Metall.* **8** (1974) 425.
32. N. S. GOLOSOV and A. M. TOLSTIK, *J. Phys. Chem. Solids* **36** (1975) 899.
33. *Idem, ibid.* **36** (1975) 903.
34. H. INO, *Acta Metall.* **26**, (1978) 827.
35. M. HASAKA, *Trans. JIM.* **21** (1980) 660.
36. H. SAGANE and K. OKI, *ibid.* **21** (1980) 811.
37. H. KUBO and C. W. WAYMAN, *Acta Metall.* **28** (1980) 395.
38. H. KUBO, *J. Phys. Chem. Solids* **44** (1983) 323.
39. G. INDEN, *Physica.* **103B** (1983) 82.
40. W. L. BRAGG and E. J. WILLIAMS, *Proc. Roi. Soc.* **A145** (1934) 699.
41. V. S. GORSKY, *Z. Physik.* **50** (1928) 64.
42. G. INDEN, *Phys Status Solidi* **56** (a) (1979) 177.

Received 17 October 1988
accepted 13 April 1989